Synthesis, crystal structure, spectral, thermal, dielectric, z-scan analysis and computational studies of 8-hydroxyquinolinium trichloroacetate (8HQTC)

E. Shobhana [a,*], R. Kesavasamy [b], B. Babu [c], R. Karunathan [d]
[a]*Department of Physics,School of Foundational Science, Kumaraguru College of Technology, Coimbatore-641 049, Tamilnadu, India.*
[b]*Department of Physics, Sri Ramakrishna Engineering College, Coimbatore-641 022, Tamilnadu, India.*
[c] *Department of Electrical Engineering, National Tsing Hua University, Hsinchu City - 30013, Taiwan*
[d] *Department of Physics, Dr.NGP Arts and Science College, Coimbatore, Tamil Nadu, India*

An organic third-order nonlinear optical single crystal of 8-hydroxyquinolinium trichloroacetate (8HQTC) has been broughten about by proton transfer reaction established by slow evaporation method. Single crystal X-ray diffraction analysis profoundly revealed the crystal structure of 8HQTC in monoclinic system with the space group of C2/c. 8-hydroxyquinolinium (8HQ+) cations are linked to trichloroacetate (TCA^-) anions forming an ion pairs through these hydrogen atoms H6 of N1 and H5 of O1 in the form of N1—H6···O3 and O1—H5···O3 intermolecular hydrogen bonds in the unit cell that produce ring $R_4^2(14)$ motif. The vibrational (FTIR and FT-Raman)andopticaltransmittance(UV-Vis-NIR) spectral analysis were efficaciously carried out for 8HQTC crystal. TG-DTA analysis of grown material revealed the thermal stability upto 140 °C. The Frequency and temperature dependent dielectric constant and dielectric loss of the grown crystal was analysed. The nonlinear optical properties such as nonlinear refractive index (n_2=8.36 x 10^{-12} m^2/W), nonlinear absorption coefficient (β=5.69 x 10^{-6}) and third order susceptibility ($\chi^{(3)}$= 4.51 x 10^{-5} esu) values have been calculated for grown 8HQTC crystal using Z-scan measurements. The correlation between molecular structure of 8HQTC and its molecular perspectives has been accomplished by density functional theory (DFT) method.

(Received October 28, 2020; Accepted March 29, 2022)

Keywords: Crystal growth, X-ray diffraction, Thermogravimetric analysis, Dielectric properties, Optical properties

1. Introduction

Crystal engineering of self-assembled nonlinear optical materials have attained an interest among researchers reliable to its importance in the areas of lasers, optical data storage and information processing systems. [1]. NLO phenomena extensively utilized in propounding the behaviour of nonlinear coupling of electromagnetic waves which leads to the generation of terahertz radiation, second harmonic generation, optical mixing, optical limiting, and optical parametric oscillation [2-3]. In recent years, NLO perspectives has been widely studied on crystals, polymers, liquid crystals, semiconductors and organics [4]. In which organic single crystals dominated in the field of NLO materials owing to its fascinating properties over other materials like inorganics and semi-organics [5-6]. The attracting properties of organic NLO materials are large nonlinear optical susceptibility ($\chi^{(2)}$), low dielectric constant (ε_r) at higher frequencies, laser damage tolerance (LDT) for high power laser, synthetic flexibility and easier in device fabrication [7]. On basis of these above facts, recent literature showed remarkable properties of some organic NLO crystals with the admiring properties and largely contributed to the development of organic NLO materials [8-10]. On this context, investigation of basic moiety

* Corresponding author: physhobhy@gmail.com
https://doi.org/10.15251/DJNB.2022.171.369

largely involved in synthesis of some novel NLO materials become inevitable task in this field. In this particular, quinoline derived compounds have been extensively studied and some single crystals were reported earlier with acentric crystal packing with optimum SHG efficiency [11-12]. These facts increased remarkable attention towards synthesizing of a promising new ionic quinolinium compounds with acentric crystal packing to obtain superior optical nonlinearity. In this work, a quinoline derivative of 8-hydroxyquinoline (8-HQ) was chosen to synthesize a novel ionic compound and successively grow into single crystals. Because 8-HQ (C_9H_7NO) is a quinoline-based aromatic heterocyclic compound and crystallized into noncentrosymmetric , Fdd2, orthorhombic, space group [13].Single crystals of 8-HQ were grown into large size using different solvents and revealed promising SHG efficiency of 4.2 times relative to the standard KDP material [14-16]. Furthermore, it is a well-known base molecule and an efficient chelating agent for inorganic compounds including tris(8-hydroxyquinoline) aluminum (Alq_3) a promising White-Light-Emitting Diode (WLED) [17]. In this present work, 8-hydroxyquinoline was complexed with trichloroacetic acid and formed a new ionic quinolinium single crystal, 8-hydroxyquinolinium trichloroacetate (8QTC). The grown crystal was experimentally investigated by single crystal X-ray diffraction (SCXRD), vibrational (FTIR and FT-Raman), Optical (UV-Vis-NIR), Dielectric studies and thermal (TG-DTA) studies. The third-order NLO susceptibility ($\chi^{(3)}$) value for 8HQTC crystal has been achieved by Z-scan technique.

2. Experimental

2.1. Preparation of 8HQTC compound

The AR grade compounds of 8-hydroxyquinoline (8HQ) and trichloroacetic acid (TCA) were procured from Alfa Aesar with ≥ 99.0 % purity for synthesis of 8HQTC compound. 8HQ (0.725 g, 0.5 mol) and TCA (0.816 g, 0.5 mol) compounds were taken in (1:1) equimolar ratio and dissolved by 10 ml of ethanol and double distilled water independently using constant strirring for 30 minutes at 40 °C. The chemical scheme of synthesis is illustrated in Fig.1a. The prepared solutions were combined together and stirred for about 100 minutes at room temperature. The mixture solution was successively transformed into appropiate sized petri dish after filtration using Whatman grade-1 filter paper. The evaporation was controlled effectively by covering the solution by a tiney holed transparent polythene paper. The single crystals of 8HQTC with diffraction quality has been harvested from the solution after 6 days. The photograph of as-grown single crystal of 8HQTC is illustrated in Fig.1b.

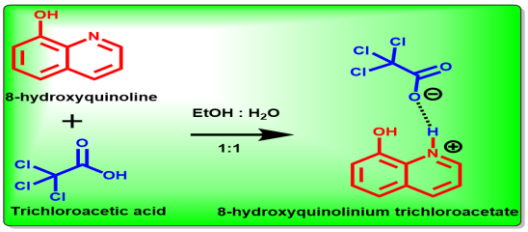

Fig. 1. a.The chemical scheme synthesis of the 8HQTC crystal.

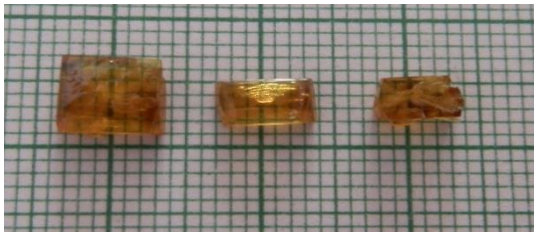

Fig. 1. b. The grown single crystal of 8HQTC.

2.2. Characterization techniques

The KBr pelletization method was employed to report the FTIR spectra for 8HQTC compound using Shimadzu IRAffinity-1S FTIR spectrometer. The FTIR spectra was recorded with a resolution of 0.5 cm^{-1} in the spectral range of 4000-400 cm^{-1}. FT-Raman spectra was recorded by Nd:YAG laser with a wavelength of 1064 nm as excitation source used BRUKER RFS27: standalone FT-Raman spectrometer. UV-Vis-NIR optical transmittance spectra was performed using Perkin-Elmer Lambda 35 Spectrophotometer with the resolution of ±0.05 nm in the wavelength range between 200 and 1500 nm. Perkin Elmer Simultaneous Thermal Analyzer (STA) 8000 has been utilized to perform thermogravimetric and differential thermal analysis measurements simultaneously in the temperature range between from 50 °C to 900 °C at a heating rate of 20 °C /min. Enraf Nonius CAD-4 single crystal X-ray diffractometer has been used for collecting diffraction data. Where graphite monochromated Mo Kα X-ray source (λ = 0.7104 °) was employed for diffraction using ω-2θ scan method. The structrual determination has been carried out by SHELXS-97 program [18] where direct method procedures were employed. The structural refinement was made using for all the non-hydrogen atoms by anisotropic least square refinement method employing SHELXL-97 program [18]. The thermal displacement ellipsoids (ortep), intermolecular interactions (graph set motifs) and unitcell packing diagrams were depicted using Ortep- 3 [19], Mercury-3.8 software [20] and Diamond software [21] respectively.

2.3. Computaional Studies

Density functional theory has been extremely employed for organic molecules owing to its computational accuracy reliable with the experimental results. In this work, complete computational calculations were performed for 8HQTC molecule by density functional theory (DFT) in ground state using Gaussian 03 program package [22]. The molecular geometry optimization was performed inorder to achieve energy minimized title molecule for calculating its properties at molecular level using Hybrid, Becke three (B3) parameters exchange and Lee-Yang-Par (LYP) functional with 6-311++G(d,p) basis set level of theory. The crystallographic internal coordinates have been utilized for generating input file for molecular structure optimization. The minimized energy value for 8HQTC molecule is -2084.99 a.u and the optimized structure is shown in Fig.2. with the labelling scheme. The molecular geometrical comparison has been performed between X-ray crystal structure and calculated structure. The geometrical parameters including bond distances, bond angles and dihedral angles has already been tabulated in Table 3. The root mean square deviation (RMSD) has been calculated between experimental and compuational structure. The estimated RMSD values are 0.01 Å, 0.46 ° and 2.20 ° for bond distances, bond angles and dihedral angles, respectively. The determined values of RMSD value obviously confirmed the admirable agreement between experimental and calculated molecular geometry.

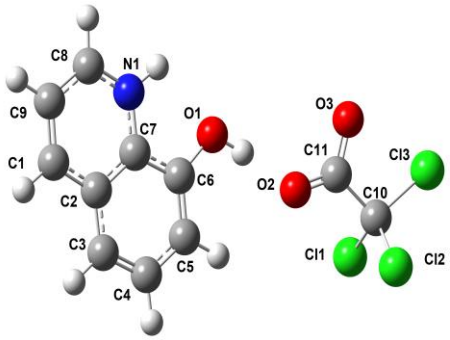

Fig. 2. The optimized structure of 8HQTC.

3. Results and discussions

3.1. Crystal structure analysis

The title crystal was crystallized into monoclinc, centrosymmetric space group of C2/c with the unit cell parameters (a = 18.612(5) Å, b = 5.774(5) Å, c = 23.543(5) Å, β = 92.746(5)° and Z= 4). The crystallographic structural refinement details were tabulated in Table 1. The geometry of some selected hydrogen bonds observed for 8HQTC crystal has been tabulated in Table 2. The crystal structure of 8HQTC($C_{11}H_8Cl_3N_1O_3$) contained one protonated 8-hydroxyquinoline ($C_9H_8NO^+$) molecule, exist in cationic form, and one deprotonated trichloroacetic acid ($C_2Cl_3O_2^-$) molecule, exist in anionic form. The molecular structure of 8HQTC crystal derived from the X-ray diffraction analysis along with the atom numbering scheme is depicted in Fig 3a. 8HQ was protonated at endocyclic N-site of the ring. The most significant changes occurred in the C(7)-N(1)-C(8) angle, which increased by about 3° (C7—N1—C8 bond angle of 122.66(2)°) upon protonation when compared with 119.03° observed in neutral 8HQ moiety [13]. Protonation also modified bond lengths of C7—N1 and C8—N1 (Table S1) within the 8HQ ring. The observed changes in the bond distances and bond angle were good agreement with the bond distances and bond angle found in the maleic acid, fumaric acid and succinic acid salts of 8-Hydroxyquinoline cations [12-13]. It was explicitly observed that carboxyl hydrogen atoms were fully deprotonated and there was a proton–transfer process from TCA to 8HQ as shown in Fig. 3a. The observed variation in C(11)–O(2) bond length in Table 3 at the carboxylic acid of TCA corroborated the deprotonation undoubtedly. The C–Cl bond lengths observed in TCA^- found to be good agree with the C–Cl bond length values reported in 2-Carboxypyridin-1-ium trichloroacetate [23]. The 8HQ cation is structurally planar with the r.m.s deviation of 0.086. The dihedral angle between the cation and anion is 88.99(3) ° which indicated that they were almost perpendicular to each other. In this crystal structure (8HQTC) trichloroacetate anion played a vital role in formation of intermolecular hydrogen bonds with the 8-hydroxyquinolinium cation via H atoms in NH^+ and OH groups. The cations linked to anions forming an ion pairs through these hydrogen atoms H6 of N1 and H5 of O1 in the form of N1—H6···O3 and O1—H5···O3 intermolecular hydrogen bonds in the unit cell that produced a ring $R_4^2(14)$ motif is shown in Fig. 3b [24]. The 3-dimensional graphical illustration of crystal packing for 8HQTC is depicted in Fig. 3c viewing along a axis. The O—H···O intermolecular hydrogen bond was almost linear (angle O—H···O = 177.52(2) °) with an O—H distance of 0.757(2) Å and an O···O distance of 2.75(2) Å, corresponding to the normal hydrogen bond. The crystal structure of 8HQTCA was determined to be stabilized by the network of N—H···O and O—H···O intermolecular hydrogen bonds.

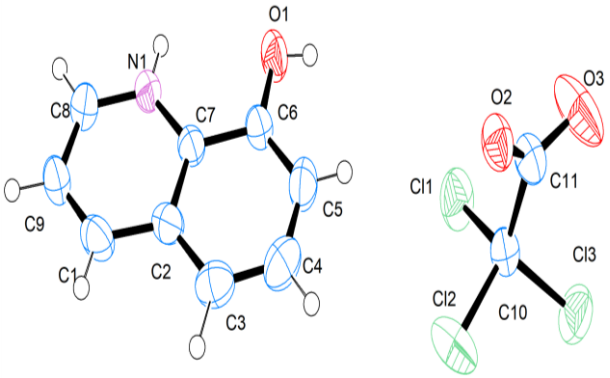

Fig. 3. a.The atom numbering scheme of 8HQTC crystal.

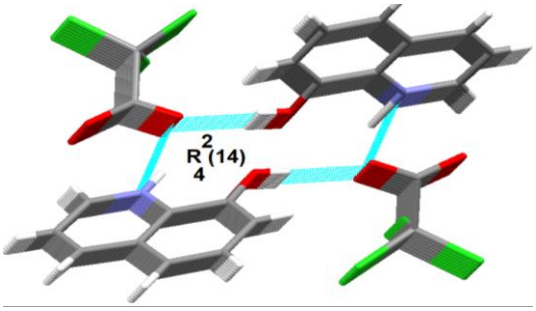

Fig. 3.b. The ring $R_4^2(14)$ motif of 8HQTC crystal.

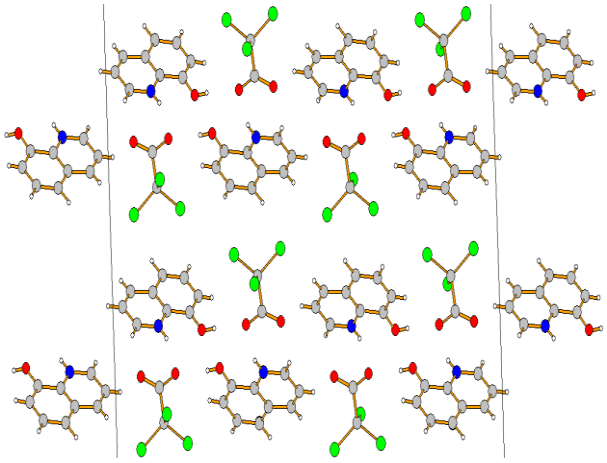

Fig. 3. c. The 3-dimensional graphical illustration crystal packing of the grown crystal.

Table 1. Crystal data and structure refinement for 8HQTC.

Empirical formula	C_{11} H_8 Cl_3 N_1 O_3	
Formula weight	308.53	
Temperature	293(2) K	
Wavelength	0.71069 Å	
Crystal system	monoclinic	
Space group	C2/c	
Unit cell dimensions	a = 18.612(5) Å	α = 90 °.
	b = 5.774(5) Å	β = 92.746(5)°.
	c = 23.543(5) Å	γ = 90 °.
Volume	2527(2) $Å^3$	
Z	4	
Density (calculated)	1.622 Mg/m^3	
Absorption coefficient	0.723 mm^{-1}	
F(000)	1248	
Crystal size	0.32 x 0.30 x 0.28 mm^3	
Theta range for data collection	2.19 to 24.97°.	
Index ranges	0≤h≤22, -1≤k≤6, -27≤l≤27	
Reflections collected	2764	
Independent reflections	2214 [R(int) = 0.0166]	
Completeness to theta = 24.97°	99.8 %	
Refinement method	Full-matrix least-squares on F^2	
Data / restraints / parameters	2214 / 0 / 196	
Goodness-of-fit on F^2	1.049	
Final R indices [I>2σ(I)]	R1 = 0.0384, wR2 = 0.1027	
R indices (all data)	R1 = 0.0458, wR2 = 0.1096	
Largest diff. peak and hole	0.424 and -0.285 $e.Å^{-3}$	
CCDC Number	947530	

Table 2. Some selected intermolecular hydrogen bonds for 8HQTC [Å and º].

D-H...A	d(D-H)	d(H···A)	d(D···A)	<(DHA)
N(1)—H(6)···O(1)#1	0.89(3)	2.40(3)	2.69(3)	99.94(2)
N(1)—H(6)···O(2)#2	0.89(2)	2.98(3)	3.43(4)	113.67(2)
C(8)—H(7)···O(2)#2	0.95(3)	2.25(3)	3.08(4)	144.58(3)
N(1)—H(6)···O(3)#2	0.89(2)	1.99(3)	2.84(2)	159.71(2)
C(5)—H(4)···O(1)#3	0.85(3)	2.89(3)	3.25(4)	107.25(3)
O(1)—H(5)···O(3)#4	0.78(4)	2.00(2)	2.76(3)	177.51(4)

Symmetry transformations used to generate equivalent atoms:
(#1) x,y,z
(#2) x,+y+1,+z
(#3) -x+1/2,+y-1/2,-z+1/2
(#4) -x+1/2,+y+1/2,-z+1/2

Table 3. Bond lengths, bond angles and dihedral angles comparison between XRD and DFT optimized structure of 8HQTC.

Atoms	(XRD)	6311++G(d,p)
Bond length values (Å)		
Cl(3)-C(10)	1.766(2)	1.806
Cl(1)-C(10)	1.774(3)	1.774
Cl(2)-C(10)	1.772(2)	1.774
C(7)-N(1)	1.369(3)	1.370
C(7)-C(2)	1.416(3)	1.422
C(7)-C(6)	1.421(3)	1.416
O(3)-C(11)	1.245(3)	1.278
O(1)-C(6)	1.350(3)	1.346
N(1)-C(8)	1.328(3)	1.334
C(6)-C(5)	1.369(4)	1.381
C(11)-O(2)	1.222(3)	1.224
C(11)-C(10)	1.578(3)	1.538
C(5)-C(4)	1.399(4)	1.381
C(2)-C(3)	1.412(4)	1.416
C(2)-C(1)	1.417(4)	1.413
C(8)-C(9)	1.396(4)	1.395
C(9)-C(1)	1.359(4)	1.383
C(3)-C(4)	1.366(4)	1.376
Bond angle values (°)		
N(1)-C(7)-C(2)	119.2(2)	119.04
N(1)-C(7)-C(6)	120.1(2)	119.13
C(2)-C(7)-C(6)	120.6(2)	121.83
C(8)-N(1)-C(7)	122.6(2)	123.41
O(1)-C(6)-C(5)	125.8(2)	126.83
O(1)-C(6)-C(7)	115.9(2)	115.08
C(5)-C(6)-C(7)	118.2(2)	118.08
O(2)-C(11)-O(3)	129.0(2)	120.53
O(2)-C(11)-C(10)	114.1(2)	124.27
O(3)-C(11)-C(10)	116.8(2)	115.20
C(6)-C(5)-C(4)	121.3(3)	120.51
C(3)-C(2)-C(7)	119.0(2)	118.36
C(3)-C(2)-C(1)	123.8(2)	124.38
C(7)-C(2)-C(1)	117.1(2)	117.26
N(1)-C(8)-C(9)	120.3(3)	119.80

C(11)-C(10)-Cl(3)	113.68(7)	104.29
C(11)-C(10)-Cl(2)	110.34(6)	109.39
Cl(3)-C(10)-Cl(2)	107.95(3)	110.94
C(11)-C(10)-Cl(1)	107.08(7)	109.31
Cl(3)-C(10)-Cl(1)	109.18(3)	110.96
Cl(2)-C(10)-Cl(1)	108.50(3)	109.39
C(1)-C(9)-C(8)	119.3(2)	119.32
C(4)-C(3)-C(2)	119.3(2)	119.31
C(9)-C(1)-C(2)	121.3(2)	121.17
C(3)-C(4)-C(5)	121.6(3)	121.91
Torsion angle values (°)		
C(2)-C(7)-N(1)-C(8)	-1.2(3)	0.00
C(6)-C(7)-N(1)-C(8)	178.3(2)	179.99
N(1)-C(7)-C(6)-O(1)	-0.1(3)	0.02
C(2)-C(7)-C(6)-O(1)	179.4(2)	179.98
N(1)-C(7)-C(6)-C(5)	179.6(2)	179.97
C(2)-C(7)-C(6)-C(5)	-0.9(3)	0.03
O(1)-C(6)-C(5)-C(4)	-178.8(3)	-179.98
C(7)-C(6)-C(5)-C(4)	1.5(4)	-0.04
N(1)-C(7)-C(2)-C(3)	179.3(2)	179.99
C(6)-C(7)-C(2)-C(3)	-0.2(3)	0.00
N(1)-C(7)-C(2)-C(1)	-0.4(3)	-0.01
C(6)-C(7)-C(2)-C(1)	-179.9(2)	-180.00
C(7)-N(1)-C(8)-C(9)	1.5(4)	0.01
O(2)-C(11)-C(10)-Cl(3)	162.0(2)	165.21
O(3)-C(11)-C(10)-Cl(3)	-19.3(3)	-17.86
O(2)-C(11)-C(10)-Cl(2)	40.6(3)	42.48
O(3)-C(11)-C(10)-Cl(2)	-140.8(2)	-139.59
O(2)-C(11)-C(10)-Cl(1)	-77.3(3)	-76.08
O(3)-C(11)-C(10)-Cl(1)	101.3(2)	103.86
N(1)-C(8)-C(9)-C(1)	-0.2(4)	0.00
C(7)-C(2)-C(3)-C(4)	0.8(4)	-0.02
C(1)-C(2)-C(3)-C(4)	-179.5(3)	-179.98
C(8)-C(9)-C(1)-C(2)	-1.4(4)	0.00
C(3)-C(2)-C(1)-C(9)	-178.0(3)	-179.99
C(7)-C(2)-C(1)-C(9)	1.7(4)	0.01
C(2)-C(3)-C(4)-C(5)	-0.2(4)	0.01
C(6)-C(5)-C(4)-C(3)	-1.0(4)	0.02

3.2 FTIR and FT-Raman vibrational analysis

The position of intermolecular interactions in vibrational spectra mainly depends on its strength. X-ray structural investigation edivently confirmed that $8HQ^+$ cation and TCA^- anion has been connected through N─H···O intermolecular interactions. The N─H···O stretching vibration typically expected to appears in the region of 2100-1870 cm^{-1} and mostly appears in IR spectrum. FTIR frequencies with their vibrational assignments of 8HQTC compound is tabulated in Table 4. In Fig.4, A weak intensity peak at 2094 cm^{-1} has been observed in FTIR spectrum corresponding to this vibration. Generally the peaks corresponding to aromatic C-H stretching mode appears in the region of 3100-2900 cm^{-1} [25]. Accordingly, 8HQTC compound showed a weak intensity peak at 3055 cm^{-1} in FTIR spectra and a strong intensity peak at 3066 cm^{-1} in Raman spectra. The C-N stretching vibration was noticed by the presence of a peak at 1635(w) cm^{-1} and 1629(m) cm^{-1} in FTIR spectra and FT-Raman spectrum, respectively. A medium intensity peak appeared at 1558 cm^{-1} is owing to the C-O stretching mode found in $8HQ^+$ [12]. The deformation mode of O-H vibration has been observed around 1473 cm^{-1}. The peaks appeared at 1308(s), 1139(w) and 1095(m) cm^{-1} in FTIR spectra and 1295(s), 1139(w) cm^{-1} in Raman spectra are assigned to aromatic C-H in plane bending vibrational modes. The aromatic C-H out of plane bending

vibrations appeared as weak intensity peaks at 949 and 911 cm^{-1} in FTIR spectra of 8-HQTC compound.

The asymmetric and symmetric stretching vibrational modes of carboxylate functional group attached to the TCA^- anion has been noticed at 1598(s), 1400(w) cm^{-1} in FTIR spectra and 1607(s), 1398(s) cm^{-1} in Raman spectra, respectively. A medium intensity peak at 1673 cm^{-1} (FTIR) and a weak intensity peak at 1674 cm^{-1} (FT-Raman) is ascribed to the C=O stretching vibration of the non-ionized carboxylic acid group attached to TCA^- anion. The deformation vibrations of carboxylate group such as rocking, scissoring and wagging have been identified at 709(w), 669(s) and 418(w) in FTIR spectra and at 707(s), 668(w) and 423(s) cm^{-1} in FT-Raman spectra of 8-HQTC compound. Medium intensity peak at 830 cm^{-1} in infrared spectra and a weak counterpart in Raman spectra at 824 cm^{-1} were attributed to the C-C stretching vibration [27]. The C-Cl stretching vibration produced a weak intensity peak at 741 cm^{-1} in FTIR spectra and a medium counterpart at 736 cm^{-1} in Raman spectra [26].

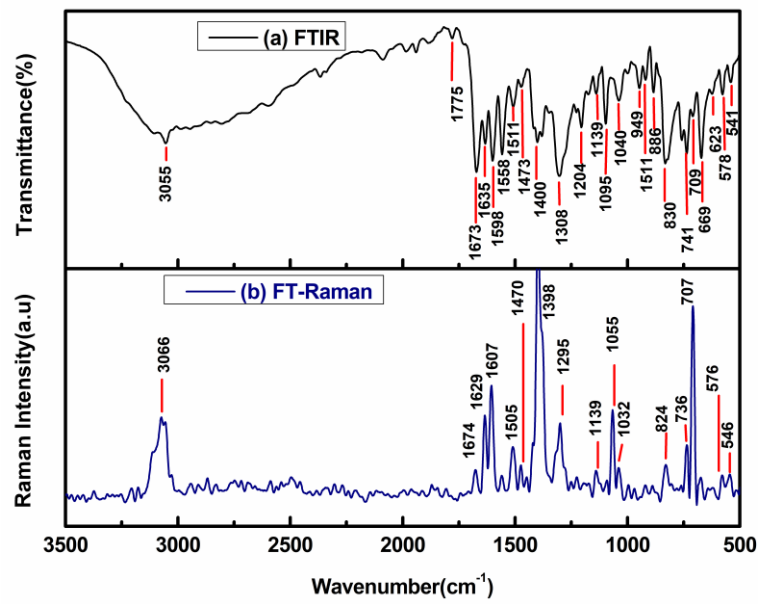

Fig. 4.The FTIR and FT-Raman vibrational assignments of 8HQTC crystal

Table 4. FTIR frequencies with their vibrational assignments of 8HQTC compound.

FTIR (cm^{-1})	FT-Raman (cm^{-1})	mode of vibrations
3055(w)	3066(s)	ν(C-H)
2094(w)		ν(N⋯H⋯O)
1775(W)		ν(C=O)
1673(m)	1674(w)	ν(C=O)
1635(w)	1629(m)	ν(C-N)
1598(m)	1607(s)	$\nu_{as}(COO^-)$
1558(m)		δ(CO)
1511(w)	1505(m)	ν(C=C)
1473(w)	1470(w)	δ(OH)
1400(w)	1398(s)	$\nu_s(COO^-)$
1308(s)	1295(s)	δ_{ipb} (CH)
1139(w)	1139(w)	δ_{ipb} (CH)
1095(m)		δ_{ipb} (CH)
1040(w)	1055(s)	ω ring
949(w)		δ_{opb} (CH)
911(w)		δ_{opb} (CH)
886(w)		δ(OH)
830(m)	824(w)	ν(C-C)
741(w)	736(m)	ν(C-Cl)
709(w)	707(s)	$\rho(COO^-)$
623(w)		δ(C-Cl)
669(s)	668(w)	sci(COO^-) and δ(C-Cl)
578(w)	576(w)	δ(CO)
541(w)	546(w)	ω(C⋯C=O)
488(w)	477(m)	τ ring
418(w)	423(s)	ω(COO^-) and ν(C-Cl)

δ – deformation; ω – wagging; sci – scissoring; ρ – rocking; τ – twisting; ν –stretching; ν_s – symmetric stretching; ν_{as} – asymmetric stretching; w – weak; m – medium; s – strong; ipb-in plane bending; opb-out of plane bending.

3.3 UV-Vis-NIR optical transmittance analysis

UV-Vis-NIR spectral study was employed to explore the nature of electronic transitions and optical transparency region of grown 8HQTC crystal having thickness of 3.5 mm. These perspectives extremely associated and used to confirm the suitablity of title crystal to be employed in optical applications such as photonics and optoelectronics. The UV-Vis-NIR optical transmittance spectra was recorded for 8HQTC crystal and presented in Fig. 5. The optical spectra displayed the cut off wavelength around 400 nm corresponding to n-π* transition. This transition is owing to the electronic transition from a lone pair of electrons of electronegative (oxygen) atoms to π* electrons in the 8HQTC crystal [27]. The optical transmittance spectra revealed that grown crystal disclosed an admirable optical transparency of around 60% within the spectral region of 400-1200 nm. The spectra displayed minute absorptions around 800 and 1000 nm owing to the C-C stretching and deformation modes of C-H vibrations. The good optical transparency in visible and near IR region evidently suggested the suitability of 8HQTC crystal for optical applications.

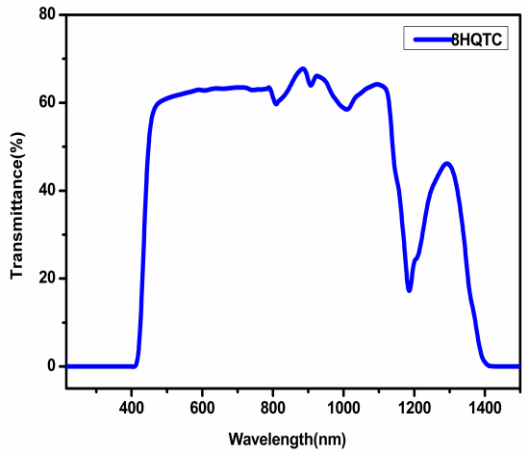

Fig.5.The UV-Vis-NIR optical transmittance spectra of 8HQTC crystal.

3.4. TG/DTA thermal analysis

The simultaneous thermogravimetric (TG) and differential thermal analysis (DTA) analysis has been employed for grown 8HQTC crystal. The experiment was performed on powder crystalline sample of title crystal having weight of 10 mg with the heating rate of 20 °C/min at room temperature. The measured TG-DTA curves of 8HQTC sample has been illustrated in Fig. 6. The thermograms showed an sharp endothermic peak at 140 °C which certainly conforming to the melting point and the sharpness associated to the purity of grown material. The TGA curve displayed three stages of decomposition gradually. A major weight loss of about 52 % has been noticed between 140-146 °C. After that second stage of decomposition has been detected between 146-263 °C which resulted in weight loss of about 40 %. The third stage of weigh loss of about 8% was observed between 260-565 °C which corroborated that all the moieties were eliminated into some gaseous products such as CO, NH_3 and CO_2 [28-29]. Hence, TG-DTA thermal analysis revelaed the thermal stablity of title crystal for applications upto 140 °C.

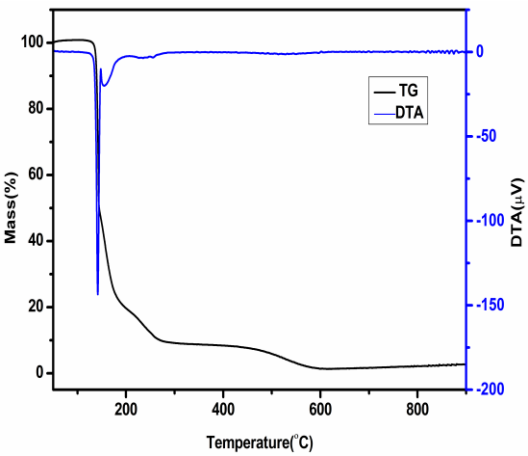

Fig. 6. The TG-DTA of 8HQTC crystal.

3.5. Dielectric studies

Defect behaviour, transport phenomena of ions under the influence of applied field and its structural behaviour can be studied using dielectric studies [30]. Dielectric constant and dielectric loss were carried out as a function of various frequencies (500Hz to 1MHz) for various temperatures (30˚C to 70˚C) on the polished surface of 8HQTC crystal. The sample with the thickness of 1.32 mm was made electrically conductive by coating silver paste on both the sides.

Fig. 7a represents the variation of dielectric constant with respect to range of frequencies. It has been clear that dielectric constant is decreasing with respect to increase in frequency as well as temperature. The high value of dielectric constant at low frequency at room temperature reflects the influence of space charge polarization due to existence of grain boundaries in crystal materials. It can be inferred, dipoles easily respond and align with applied alternate electric fields at low frequencies. As the frequency increases, the value of dielectric constant decreases due to the fact that dipoles cannot respond with highly varying electric field [31].8HQTC crystal formed through proton transfer using 8-Hydroxyquinoline and trichloroacetic acid as donor and acceptor respectively, a combination of ionic and donor-acceptor hydrogen bond interaction links the hydroxyquinoline and trichloroacetate ions to form a three dimensional network [32]. A dielectric anomaly has been observed for every temperature in frequency range of 5K Hz to 10 K Hz, which is due to the orientational polarization observed in the crystal. The orientational polarization is possible only if the molecules in the material associated with an asymmetrical structure [33]. The low dielectric constant value at higher frequency is one of the prime factors for the enhancement of SHG co-efficient. Dielectric loss was also carried as a function of frequency for the various temperatures. Dissipation of energy due to the ionic movement with respect to the applied filed can be quantified by studying dielectric loss [34]. We can infer from Fig. 7b that dielectric loss decreases with respect to increase in frequency. Dielectric loss is also exhibiting the same type of variation as observed in the dielectric constant. The lower dielectric loss at high frequencies suggests that the grown crystal is having lesser defect density, which is an important phenomenon to be an active NLO material.

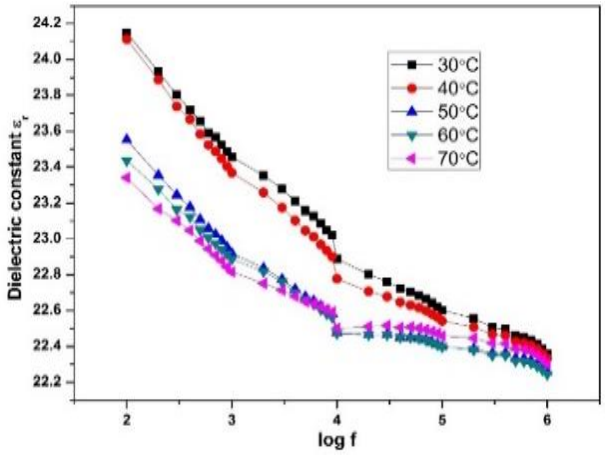

Fig. 7. a. Dielectric constant vs. log f (Hz).

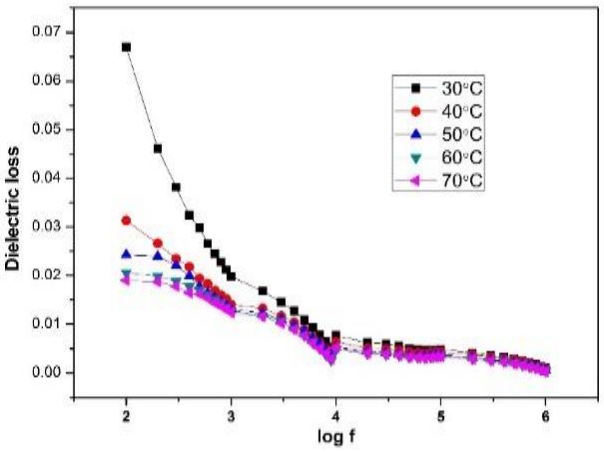

Fig. 7. b. Dielectric loss vs. log f.

3.6. Z-scan measurement

The nonlinear refractive index (n_2) with its sign and magnitude could be determined efficiently using Z-scan technique introduced by Sheik Bahae et al [35-36]. It is a unique and extremely recognized technique to be employed for gaining knowledge about nonlinear optical properties such as the nonlinear absorption coefficient(β) and the TONLO susceptibility($\chi^{(3)}$) for solids, liquids and thin films. The 8HQTC crystal was subjected to Z-scan measurement by He-Ne laser (λ= 632.8 nm) as an excitation source with the beam diameter of 0.5 mm. The Gaussian beam was generated by focusing the laser beam into Gaussian filter. The output (Gaussian) beam TEM_{00} mode has been proceeded via a convex lens with a focal length of 30mm. The intensity of the input beam was adjusted by translating the sample across in the +Z to -Z axial direction. The digital power meter (Field master GS-coherent) was employed for measuring the variations in the far field intensity through the closed aperture. The normalized transmittances (T) were noted with respect to the closed and open aperture conditions as a function of distance Z along the lens axis. The curves of open and closed aperture were shown in Fig.8a and 8b respectively. The results of closed aperture for title crystal showed the positive value of TONLO refractive index (n_2). The positive nonlinear refractive index is the result of self-focusing nature owing to the two-photon absorption nature of title crystal. The nonlinear refractive index(n_2), nonlinear absorption coefficient(β) and third order susceptibility($\chi^{(3)}$) values were calculated as 8.36 x 10^{-12} m^2/W, 5.69 x 10^{-6} m/W and 4.51 x 10^{-6} esu using the equations (20–30) reported by Senthil et al., 2014 [36]. The determined TONLO susceptibility ($\chi^{(3)}$) value of 8HQTC crystal was comparable with some TONLO materials reported earlier such as BTZB [38] and BTZA [39]. The feature of self-focussing and two-photon absorption strongly confirmed the efficient candidature of 8HQTC crystal towards optical limiting applications [40].

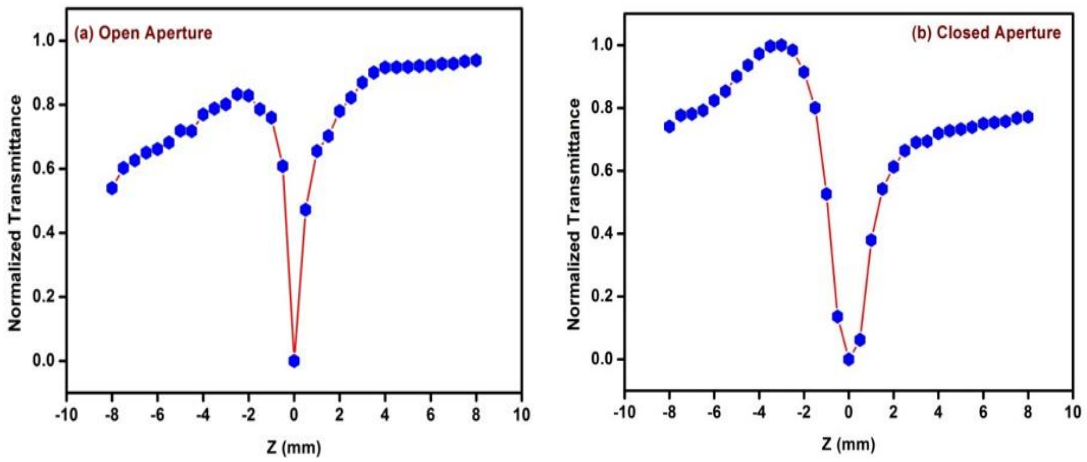

Fig. 8. a and 8b. The open and closed aperture of 8HQTC crystal.

4. Conclusion

An organic third-order nonlinear optical material of 8-hydroxyquinolinium trichloroacetate (8HQTC) has been achieved by slow evaporation method. The crystal structure has been determined in monoclinic system with centrosymmetric space group of C2/c. Vibrational signature of functional groups present in 8HQTC crystal has been identified using FTIR and FT-Raman spectral studies. The very good optical transmittacne up to 60% with in the wavelength region of 400-1500 nm for title crystal. The thermal stability up to 140 °C and endothermic decomposition has been observed. The lower dielectric loss at high frequencies suggests that the grown crystal is having lesser defect density, which is an important phenomenon to be an active NLO material. The positive nonlinear refractive index confirmed the process of two-photon absorption which evidently suggested that 8HQTC would be a suitable crystal for optical limiting applications in near future.

Acknowledgements

The author E. Shobhana greatfully acknowledge Kumaraguru College of Technology, Coimbatore-641 049 and R. Kesavasamy thanks Sri Ramakrishna Engineering College, Coimbatore-641 022, Tamilnadu, India, for their constant support and encouragement.

References

[1] D. S. Chemla, J. Zyss, Nonlinear Optical Properties of Organic Molecules and Crystals, first edn., Academic Press, New York, 40, 1987.

[2] W. Nie, Optical Nonlinearity: Phenomena, applications, and materials 5, 520 (1993); https://doi.org/10.1002/adma.19930050704

[3] S. Chidambaram, A. D. K. Raj, R. Manimekalai, Appl. Phys. A 126, 430 (2020); https://doi.org/10.1007/s00339-020-03605-3

[4] O. Ostroverkhova, Chem. Rev. 116, 13279 (2016); https://doi.org/10.1021/acs.chemrev.6b00127

[5] C. Reese, M. Roberts, M. Ling, Z. Bao,Organic thin film transistors Materials Today 7, 20 (2004); https://doi.org/10.1016/S1369-7021(04)00398-0

[6] C. D. Dimitrakopoulos, P. R .L. Malenfant, Adv. Mater. 14, 99 (2002). https://doi.org/10.1002/1521-4095(20020116)14:2<99::AID-ADMA99>3.0.CO;2-9

[7] N. Karuppanan, S. Kalainathan, J. Phys. Chem. C 122, 4572 (2018); https://doi.org/10.1021/acs.jpcc.7b11884

[8] J.-H. Jeong, B.-J. Kang, J.-S. Kim, M. Jazbinsek, S.-H. Lee, S.-C. Lee, I.-H. Baek, H. Yun, J. Kim, Y.S. Lee, J.-H. Lee, J.-H. Kim, F. Rotermund, O.-P. Kwon, Sci. Rep. 3, 3200 (2013); https://doi.org/10.1038/srep03200

[9] P. J. Kim, J. H. Jeong, M. Jazbinsek, S. B. Choi, I. H. Baek, J. T. Kim, F. Rotermund, H. Yun, Y. S. Lee, P. Günter, O.P. Kwon, Adv. Funct. Mater. 22, 200 (2012); https://doi.org/10.1002/adfm.201101458

[10] R. Rajkumar, P. Praveen Kumar, Appl. Phys. A 124, 382 (2018); https://doi.org/10.1007/s00339-018-1783-2

[11] G. Peramaiyan, P. Pandi, N. Vijayan, G. Bhagavannarayana, R. Mohan Kumar, J. Cryst. Growth 375, 6 (2013); https://doi.org/10.1016/j.jcrysgro.2013.04.011

[12] R. Thirumurugan, B. Babu, K. Anitha, J. Chandrasekaran, Spectrochim. Acta - Part A Mol. Biomol. Spectrosc. 140, 44 (2015); https://doi.org/10.1016/j.saa.2014.12.093

[13] Roychowdhury, Acta Cryst. B 34, 1047 (1978); https://doi.org/10.1107/S0567739478002156

[14] V. Krishnakumar, R. Nagalakshmi, P. Janaki, Spectrochim. Acta A: Mol. Biomol. Spectrosc. 61, 1097 (2005); https://doi.org/10.1016/j.saa.2004.06.029

[15] M. Rajasekaran, P. Anbusrinivasan, S.C. Mojumdar, J. Therm. Anal. Calorim. 100, 827 (2010); https://doi.org/10.1007/s10973-010-0761-5

[16] S. P. Prabhakaran, R. Ramesh Babu, P. Velusamy, K. Ramamurthi, Mater. Res. Bull. 46, 1781 (2011); https://doi.org/10.1016/j.materresbull.2011.08.001

[17] C. Pérez-Bolívar, S. Y. Takizawa, G. Nishimura, V. A. Montes, P. Anzenbacher, Chem. - A Eur. J. 17, 9076 (2011); https://doi.org/10.1002/chem.201100707

[18] G. M. Sheldrick, SHELXS97, Program for crystal structure solution. University of Gottingen, Germany, G. M. Sheldrick SHELXL97, Program for crystal structure refinement, University of Gottingen, Germany, (1997).

[19] L. J. Farrugia, J. Appl. Crystallogr. 45, 849 (2012); https://doi.org/10.1107/S0021889812029111

[20] C. F. Macrae, I. J. Bruno, J. A. Chisholm, P. R. Edgington, P. McCabe, E. Pidcock, L.

Rodriguez-Monge, R. Taylor, J. Van De Streek, P. A. Wood, J. Appl. Crystallogr. 41, 466 (2008); https://doi.org/10.1107/S0021889807067908

[21] H. Putz, K. Brandenburg, Kreuzherrenstr. 102, 53227 (1999).

[22] M. J. Frisch, G. W. Trucks, H. B. Schlegel, G. E. Scuseria, M. A. Robb, J. R. Cheeseman, J. A. Montgomery, Jr., T. Vreven, K. N. Kudin, J. C. Burant, J. M. Millam, S. S. Iyengar, J. Tomasi, V. Barone, B. Mennucci, M. Cossi, G. Scalmani, N. Rega, G. A. Petersson, H. Nakatsuji, M. Hada, M. Ehara, K. Toyota, R. Fukuda, J. Hasegawa, M. Ishida, T. Nakajima, Y. Honda, O. Kitao, H. Nakai, M. Klene, X. Li, J. E. Knox, H. P. Hratchian, J. B. Cross, V. Bakken, C. Adamo, J. Jaramillo, R. Gomperts, R. E. Stratmann, O. Yazyev, A. J. Austin, R. Cammi, C. Pomelli, J. W. Ochterski, P. Y. Ayala, K. Morokuma, G. A. Voth, P. Salvador, J. J. Dannenberg, V. G. Zakrzewski, S. Dapprich, A. D. Daniels, M. C. Strain, O. Farkas, D. K. Malick, A. D. Rabuck, K. Raghavachari, J. B. Foresman, J. V. Ortiz, Q. Cui, A. G. Baboul, S. Clifford, J. Cioslowski, B. B. Stefanov, G. Liu, A. Liashenko, P. Piskorz, I. Komaromi, R. L.Martin, D. J. Fox, T. Keith, M. A. Al-Laham, C. Y. Peng, A. Nanayakkara, M. Challacombe, P. M. W. Gill, B. Johnson, W. Chen, M. W. Wong, C. Gonzalez, J. A. Pople, Gaussian 03, Revision C.02, Gaussian, Inc., Wallingford CT, 2004.

[23] S. Gowri, K. Anitha, A. Suresh, T. Uma Devi, S. Selvanayagam, D. Sajan, A. Chandramohan, N. Lawrence, Spectrochim. Acta A: Mol. Biomol. Spectrosc. 95, 73 (2012); https://doi.org/10.1016/j.saa.2012.04.002

[24] J. Bernstein, R. E. Davis, L. Shimoni, N. Chang, Chem. Int. Ed. Engl. 34, 1555 (1995)' https://doi.org/10.1002/anie.199515551

[25] G. Socrates, Infrared and Raman Characteristic Group Frequencies-Tables and Charts, third edn.(John Wiley & Sons, Chichester, 2001).

[26] H. Tanak, K. Pawlus, M. K. Marchewka, A. Pietraszko, Spectrochim. Acta A: Mol. Biomol. Spectrosc.118, (2014); https://doi.org/10.1016/j.saa.2013.08.027

[27] K. Chaitanya, Spectrochim. Acta A: Mol. Biomol. Spectrosc. 86, 159 (2012).

[28] R. Thirumurugan, B. Babu, K. Anitha, J. Chandrasekaran, J. Mol. Struct. 1171, 915 (2018); https://doi.org/10.1016/j.molstruc.2017.07.027

[29] E. Shobhana, R.Kannan,R. Kesavasamy, B. Babu,P.Thirumoorthi, AIP Conference Proceedings, 2162, 020050 (2019); https://doi.org/10.1063/1.5130260

[30] J. Vidhya, K.Vijayakumar, C. Pari, Journal of Ovonic Research 15, 325 (2019).

[31] V. Gupta, K. K. Bamzai, P. N. Kotru, B. M. Wanklyn, Mater. Sci. Eng. B 130, 163 (2006); https://doi.org/10.1016/j.mseb.2006.03.006

[32] N. Sivakumar, N. Kanagathara, G. Bhagavannarayana, S. Kalainathan, G. Anbalagan, Journal of Crystal Growth 426, 86 (2015); https://doi.org/10.1016/j.jcrysgro.2015.05.025

[33] Chao Soo Choi, R. Venkataraman, Eun Hee Kim, Hae Sook Hwang, Sung kwon kang, Acta Crystallogr. C 60, o295 (2004); https://doi.org/10.1107/S0108270104005207

[34] H. Arul, D. Rajan Babu, R. Ezhil Vizhi, G. Bhagavannarayana, J. Cryst. Growth 423, 20 (2015); https://doi.org/10.1016/j.jcrysgro.2015.04.021

[35] M. Sheik-Bahae, A. A. Said, E. W. Van Stryland, Opt. Lett. 14, 955 (1989); https://doi.org/10.1364/OL.14.000955

[36] M. Sheik-Bahae, A. A. Said, T. H. Wei, D. J. Hagan, E. W. Van Stryland, IEEE J. of Quantum Electron 26, 760 (1990); https://doi.org/10.1109/3.53394

[37] K. Senthil, S. Kalainathan, A. Ruban Kumar, P. G. Aravindan, RSC Adv. 4, 56112 (2014); https://doi.org/10.1039/C4RA09112D

[38] T. C. Sabari Girisun, S. Dhanuskodi, D. Mangalaraj, J. Phillip, Synthesis, Curr. Appl. Phys. 11, 838 (2011); https://doi.org/10.1016/j.cap.2010.12.004

[39] G. Pabitha, R. Dhanasekaran, Opt. Laser Technol. 50, 150 (2013); https://doi.org/10.1016/j.optlastec.2013.03.004

[40]E. Shobhana, R. Kesavasamy, H. Arul, R. Thirumurugan, B. Babu, J. Mol. Struct. 1204, 127516 (2020); https://doi.org/10.1016/j.molstruc.2019.127516